Coupling and breakup effects of deuteron on $d + {}^{11}$B system*

Rehab Yajzey[1] Hamdah Taresh Alanazi[2] Awad A. Ibraheem[3†] Sh. Hamada[4]

[1]Department of Physical Sciences, Physics Division, College of Science, Jazan University, Jazan 45142, Saudi Arabia
[2]Department of Physics, ‹College of Science and Humanities› Shaqra University, Shaqra 11961, Saudi Arabia
[3]Physics Department, King Khalid University, Al-Qaraa Campus, Abha 61421, Saudi Arabia
[4]Physics Department, Faculty of Science, Tanta University, Tanta 31527, Egypt

Abstract: In the present study, we examine the reaction dynamics of the $d + {}^{11}$B system with a special focus on the interplay between deuteron breakup and nucleon transfer mechanisms. Elastic scattering data at $E_d = 21.5$ MeV are analyzed using the continuum-discretized coupled-channel (CDCC) framework to assess the role of breakup couplings. In addition, coupled-reaction-channel (CRC) calculations are performed for the ^{11}B(d, p)^{12}B neutron stripping reaction at 21.5 MeV, the ^{11}B(d, t)^{10}B neutron pickup reaction at 18 MeV, and the ^{11}B(d, ^{3}He)^{10}Be proton pickup reaction at 22 MeV. The CDCC calculations successfully reproduce the elastic angular distribution at forward angles without introducing renormalization factors, confirming the importance of continuum coupling effects. Nevertheless, deviations observed at larger angles suggest that breakup alone is insufficient. The (d, p) neutron stripping channel has negligible influence on the elastic scattering at this energy, whereas the (d, t) neutron pickup channel significantly modifies the calculated elastic cross sections over a broad angular range. The proton pickup channel produces only a minor effect. The present analysis demonstrates that neutron pickup, rather than stripping, is the primary transfer mechanism affecting $d + {}^{11}$B elastic scattering at this incident energy.

Keywords: deuteron breakup, transfer reaction, cluster folding model, CRC and CDCC methods

DOI: 10.1088/1674-1137/ae82e8 **CSTR:** 32044.14.ChinesePhysicsC.50104111

I. INTRODUCTION

As the simplest bound system of a proton and a neutron, the deuteron offers both opportunities and difficulties in the study of nuclear reactions. Its very low binding energy, merely 2.225 MeV, causes it to easily break apart into its two constituent nucleons upon interaction with a target nucleus. This property, together with its sizable spectroscopic quadrupole moment and the lack of any bound excited states, makes breakup processes especially relevant in reactions induced by deuterons. Understanding such breakup mechanisms has long been a central objective in nuclear physics, motivating the creation of advanced theoretical models.

A major advance in handling breakup effects came with the continuum-discretized coupled-channel (CDCC) method. First proposed by Rawitscher [1] and later improved by the Kyushu group [2, 3], this approach has transformed the analysis of deuteron-induced reactions. Over time, it has become a standard tool, particularly useful for studying reactions involving weakly bound exotic nuclei at low incident energies, and it is still being further developed [4]. The CDCC formalism was further extended to include higher-order continuum couplings by Summers *et al.* [5]. An alternative to CDCC is the adiabatic distorted wave approximation (ADWA) of Johnson and Tandy [6], which has been successfully applied to deuteron breakup at low energies [7]. A comprehensive review of theoretical methods for deuteron-induced reactions, including comparisons between CDCC and ADWA, is provided by Timofeyuk and Johnson [7]. Chau Huu-Tai [8] performed a broad systematic study of deuteron elastic-scattering data within the CDCC framework, confirming its validity over a wide range of target masses and incident energies. For light targets at low bombarding energies, CDCC calculations give a good account of the measured elastic angular distributions (ADs) at forward angles, indicating that breakup couplings play a key role there [8]. Nevertheless, at larger angles, noticeable deviations between theory and experiment usually appear, pointing to the need for including reaction mechanisms other than breakup. This suggests that couplings between the elastic channel and various direct-reaction channels—especially nucleon transfer—are important.

The effect of transfer reactions on elastic scattering has been studied for several years. Recent works [9−14]

Received 7 May 2026; Accepted 25 June 2026; Accepted manuscript online 26 June 2026

* This work through the Large Research Groups Program under grant number RGP2/14/47

† E-mail: awad_ah_eb@hotmail.com

have shed further light on these coupling phenomena. Kawai *et al.* [13] showed that (*d*, *p*) stripping reactions significantly alter $d+^{16}$O elastic scattering at 11 MeV, and that this influence weakens as the beam energy increases. Breakup effects also decline with increasing energy, although more slowly than transfer couplings. Upadhyay and colleagues [11] conducted a systematic study of deuteron reactions on ^{10}Be, ^{12}C, and ^{48}Ca targets across 12−71 MeV. They observed that including both deuteron breakup and (*d*, *p*) stripping couplings simultaneously gives a satisfactory description of the elastic data over that entire energy range. Benchmark comparisons among CDCC, ADWA, and Faddeev calculations have shown good agreement for deuteron elastic scattering at energies above 10 MeV/nucleon [15]. Exact Faddeev/AGS calculations by Deltuva [16] have confirmed the accuracy of CDCC for deuteron breakup at low energies.

Pickup reactions have also drawn considerable interest. Keeley and Mackintosh [10] examined d + ^{40}Ca elastic scattering at 52 MeV and observed that both (*d*, *t*) and (*d*, ^{3}He) pickup channels contribute significantly for angles above 40°. More recently, Amar *et al.* [14] have analyzed the d + ^{11}B system at 14.5 MeV, showing that deuteron breakup strongly reduces the elastic differential cross section at backward angles relative to standard optical-model predictions using single-folding potentials. Their analysis indicated that couplings to the *n*-*p* continuum states are more important than the quadrupole contribution of the deuteron ground state. At this lower energy, they observed that neutron pickup (*d*, *t*) dominates the transfer coupling effects, whereas neutron stripping (*d*, *p*) plays a much smaller role, and proton pickup (*d*, ^{3}He) is negligible. Very recently, Janseitov *et al.* [17] have performed a complementary CDCC+CRC analysis for the neighboring d + ^{13}C system at similar energies. They also concluded that breakup alone is insufficient, but observed that both (*d*, *p*) and (*d*, *n*) stripping reactions are significant, whereas neutron pickup (*d*, *t*) had only a minor effect—a difference attributable to the distinct spectroscopic amplitudes (*SA*s) of the two targets.

The present work builds on these earlier studies by offering a thorough analysis of deuteron-induced reactions on an ^{11}B target at a higher incident energy (21.5 MeV for elastic and (*d*, *p*) data). We use recently published experimental data at 21.5 MeV [18] together with earlier measurements for (*d*, *t*) [19] and (*d*, ^{3}He) [20] reactions on the same nucleus at similar energies. This study provides three new elements beyond Refs. [14,18]. First, it presents a combined CDCC+CRC analysis of the d + ^{11}B system at 21.5 MeV that includes the (*d*, *p*), (*d*, *t*), and (*d*, ^{3}He) channels on equal footing, allowing a direct comparison of their relative influence on elastic scattering. Unlike Ref. [14], which analyzed elastic data at 14.5 MeV and (*d*, *p*) data at 21.5 MeV separately, the present work uses consistent elastic and (*d*, *p*) data at the same incident energy. Second, we demonstrate that, at 21.5 MeV, the (*d*, *p*) neutron stripping channel has negligible influence on the elastic scattering, whereas the (*d*, *t*) neutron pickup channel remains dominant, consistent with the lower-energy findings of Amar *et al.* [14] at 14.5 MeV. Third, new *SA*s for the ^{12}B (2^+, 0.953 MeV) and ^{10}B (1^+, 0.718 MeV) states are extracted at this energy, providing an independent check of literature values. In addition, we correct the unphysical $3P_{1/2}$ assignment for the ^{12}B (2^+, 0.953 MeV) state used in Ref. [18] to a physically justified $1P_{1/2}$ configuration based on shell-model calculations. All the calculations reported here were performed with the **FRESCO** code [21], which allows a consistent treatment of the various reaction channels and their mutual couplings. For recent developments in CDCC and CRC methods, see *e.g.*, [22−27].

II. ROLE OF DEUTERON BREAKUP IN $d+^{11}$B ELASTIC SCATTERING

To evaluate quantitatively how the breakup of the deuteron affects the elastic-scattering ADs of the d + ^{11}B system at $E_{\rm lab}$ = 21.5 MeV, we applied the CDCC formalism. In this framework, the continuum located above the deuteron breakup threshold (2.2245 MeV) is truncated and divided into discrete momentum bins. Following the prescription of Ref. [9], we chose a bin width of Δk = 0.125 fm^{-1} and included bins up to $k_{\rm max}$= 0.625 fm^{-1}, which corresponds to a maximum excitation energy of $E_{\rm max}$ = 16.33 MeV in the *n*-*p* continuum. The convergence of the CDCC model space was systematically tested. Varying Δk from 0.1 to 0.15 fm^{-1} changed the elastic cross section by less than 2% at forward angles and less than 5% at backward angles. Increasing $k_{\rm max}$ to 0.75 fm^{-1} altered the results by less than 3%. The partial-wave expansion for the *n*-*p* continuum included L = 0 (*S*-wave) and L = 2 (*D*-wave) components; L = 1 (*P*-wave) contributions were explicitly tested and observed to be below 1% of the total breakup cross section at this energy, consistent with the findings of Yahiro *et al.* [2] for similar deuteron energies. Table 1 summarizes the converged CDCC model-space parameters. One notable advantage of the CDCC method is that it naturally produces the dynamic polarization potential (DPP) originating from couplings to continuum states, thereby giving insight into breakup effects without needing any adjustable parameters.

To construct the deuteron–target interaction, the essential ingredients are the neutron–nucleus and proton–nucleus optical potentials, ideally required at exactly half the incident deuteron energy (10.75 MeV). In practice, exact-energy potentials are not always available. For n + ^{11}B, the potential of Cookson and Locke [28] at 9.72 MeV was used. For p + ^{11}B, we employed the potential of Watson *et al.* [29] at 12 MeV, which is close to the

Table 1. CDCC model-space convergence parameters

Parameter	Value tested	Adopted value	Variation in $d\sigma/d\sigma_R$ ($\theta_{c.m.}$= 60°)
Δk (fm^{-1})	0.1, 0.125, 0.15	0.125	< 2%
k_{max} (fm^{-1})	0.5, 0.625, 0.75	0.625	< 3%
n-p continuum L	0, 1, 2	0, 2	L=1 contribution < 1%
L_{max} (projectile)	10, 12, 14	12	< 2%

required half-energy. The parameters of both nucleon potentials are listed in Table 2. These nucleon potentials are folded with the internal wave function of the deuteron using a cluster-folding technique to obtain both the real and imaginary parts of the deuteron–nucleus interaction:

$$V^{CF}(\boldsymbol{R}) = \int \left[V_{n-^{11}\mathrm{B}}\left(\boldsymbol{R}-\frac{1}{2}\boldsymbol{r}\right)+V_{p-^{11}\mathrm{B}}\left(\boldsymbol{R}+\frac{1}{2}\boldsymbol{r}\right)\right]\left|\chi_{n-p}(\boldsymbol{r})\right|^2 \mathrm{d}\boldsymbol{r}, \tag{1}$$

$$W^{CF}(\boldsymbol{R}) = \int \left[W_{n-^{11}\mathrm{B}}\left(\boldsymbol{R}-\frac{1}{2}\boldsymbol{r}\right)+W_{p-^{11}\mathrm{B}}\left(\boldsymbol{R}+\frac{1}{2}\boldsymbol{r}\right)\right]\left|\chi_{n-p}(\boldsymbol{r})\right|^2 \mathrm{d}\boldsymbol{r}, \tag{2}$$

where ($V_{n-^{11}\mathrm{B}}$ and $V_{p-^{11}\mathrm{B}}$) and ($W_{n-^{11}\mathrm{B}}$ and $W_{p-^{11}\mathrm{B}}$) are the real and imaginary components of the optical potentials for the n + ^{11}B and p + ^{11}B channels, respectively. The optimal n + ^{11}B and p + ^{11}B potentials employed in our CDCC calculations are listed in Table 2. The quantity $\chi_{n-p}(\boldsymbol{r})$ represents the deuteron internal wave function describing its cluster structure. The deuteron wave function was calculated using the Gaussian n + p binding potential of Iseri *et al.* [30]:

$$V_{n-p} = V_0 \exp -(r/r_0)^2. \tag{3}$$

Both S- and D-wave components were included, with potential depths V_0 = 72.15 MeV for the S-component and V_0 = 515.26 MeV for the D-component, and a common range parameter r_0 = 1.484 fm, following the parametrization of Lacombe *et al.* [31]. The SAs for the S- and D-components were taken as 0.9706 and 0.2410, respectively, reproducing the deuteron binding energy and quadrupole moment.

Figure 1 compares the experimental elastic ADs for d + ^{11}B at 21.5 MeV with our CDCC predictions. The solid curve shows the full CDCC result, obtained without any adjustable parameters. Consistent with earlier studies of light-ion scattering, the calculation reproduces the measured data well at forward angles up to roughly 30°. In the intermediate angular region between 30° and 60°, the theoretical predictions overestimate the measured differential cross sections, whereas a clear underestimation appears in the 60°−80° range. To isolate the specific role of breakup couplings, the dashed-dotted curve in Fig. 1 displays the outcome of a single-channel calculation (no continuum coupling) that includes only the deuteron ground state. Comparing this with the full CDCC calculation reveals that breakup couplings induce a substantial

Table 2. Optimal potential parameters adopted in the CDCC computations as well as those employed in the CRC computations for the ^{11}B(d, p)^{12}B, ^{11}B(d, t)^{10}B, and ^{11}B(d, ^{3}He)^{10}Be transfer reactions. Non-renormalized U_{eff} potential was adopted for the d + ^{11}B channel in all the performed computations.

n + ^{11}B and p + ^{11}B potentials adopted in CDCC computations									
System	V_0	r_V	a_V	W_D	r_D	a_D	V_{so}	r_{so}	a_{so}
n + ^{11}B [28]	47.1	1.31	0.66	8.38	1.26	0.48			
p + ^{11}B [29]	59.75	1.138	0.57	7.68	1.138	0.5	5.5	1.138	0.57
Potential parameters employed in the CRC computations for ^{11}B(d, p)^{12}B reaction									
	V_0	r_V	a_V	W_D	r_D	a_D	V_{so}	r_{so}	a_{so}
p + ^{12}B [33]	55.0	1.125	0.57	6.5	1.125	0.5	5.5	1.125	1.05
Potential parameters employed in the CRC computations for ^{11}B(d, t)^{10}B reaction									
	V_0	r_V	a_V	W_V	r_W	a_W	W_D	r_D	a_D
t + ^{10}B [35]	119.8	1.002	0.82	2.17	1.25	0.84	3.48	1.25	0.84
Potential parameters employed in the CRC computations for ^{11}B(d, ^{3}He)^{10}Be transfer reaction									
	V_0	r_V	a_V	W_V	r_W	a_W	W_D	r_D	a_D
^{3}He + ^{10}Be [35]	119.9	1.002	0.82	2.17	1.25	0.84	7.1	1.25	0.84

reduction in the cross section values at angles beyond 60°. This behavior mirrors observations in other systems, such as d + ^{58}Ni [2] and d + ^{11}Be [32], where single-channel calculations consistently overpredict the elastic scattering data at larger angles.

Additionally, we analyzed the same elastic data using an effective potential ($U_{\rm eff}$) derived from the microscopic CDCC calculations, as illustrated in Fig. 2. This effective potential combines the cluster-folding potential ($U_{\rm CF}$) with the DPP ($U_{\rm DPP}$), each containing real and imaginary components that respectively simulate the scattering process and account for flux absorption:

$$U_{\rm eff}(r) = U_{\rm CF}(r) + U_{\rm DPP}(r),\ U = V + W. \tag{4}$$

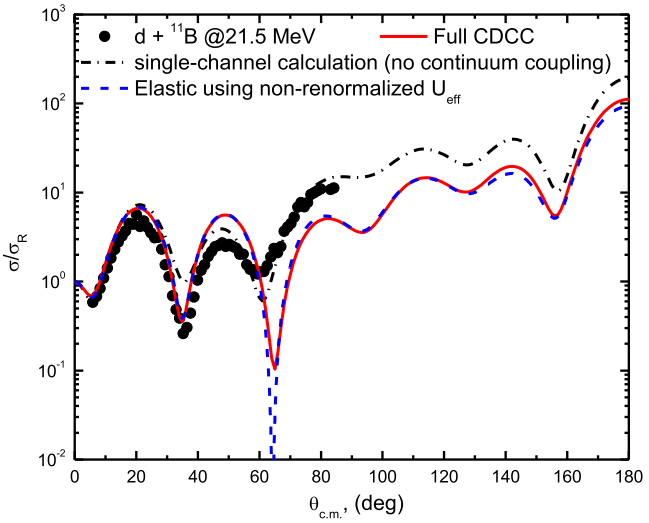

Fig. 1. (color online) Experimental d + ^{11}B elastic AD at E = 21.5 MeV (ratio to Rutherford) versus CDCC calculations (full CDCC and single-channel calculation (no continuum coupling)) and calculations within the non-renormalized $U_{\rm eff}$ potential

The $U_{\rm eff}$ is characterized by two normalization parameters, $N_{\rm Reff}$ and $N_{\rm Ieff}$, which scale the real and imaginary parts, respectively. In all the calculations presented here, these parameters were fixed at unity, maintaining the parameter-free character of the approach. The elastic scattering ADs obtained with this non-renormalized $U_{\rm eff}$ closely follow the full CDCC result, confirming the consistency between these two representations of the deuteron-target interaction.

III. ROLE OF NUCLEON TRANSFER IN d + ^{11}B ELASTIC SCATTERING

Beyond the breakup effects that manifest at lower projectile energies, additional reaction mechanisms—particularly nucleon transfer processes —can substantially modify elastic scattering angular distributions. This section examines how various transfer channels couple to the elastic channel and alter the predicted cross sections for the d + ^{11}B system.

A. Neutron-stripping transfer reaction ^{11}B(d, p)^{12}B

To investigate how neutron stripping influences the elastic scattering ADs, we analyzed previously measured ADs for the ^{11}B(d, p)^{12}B reaction at $E_{\rm d}$ = 21.5 MeV [18]. These measurements include transitions to four distinct states in ^{12}B: (1^+, 0.0 MeV), (2^+, 0.953 MeV), (2^-, 1.674 MeV), and ($J^\pi = 0^+$, 2.72 MeV). The (1^-, 2.62 MeV) and (3^-, 3.39 MeV) ^{12}B states were omitted because they are unbound or very weakly bound, requiring a more sophisticated treatment of the continuum in the exit channel, and their spectroscopic factors are small [18]; their inclusion is not expected to affect the coupling effects on elastic scattering significantly. Our CRC calculations were performed in the post form, including full complex remnant terms and non-orthogonality corrections as implemented in **FRESCO** code, following the same conventions as

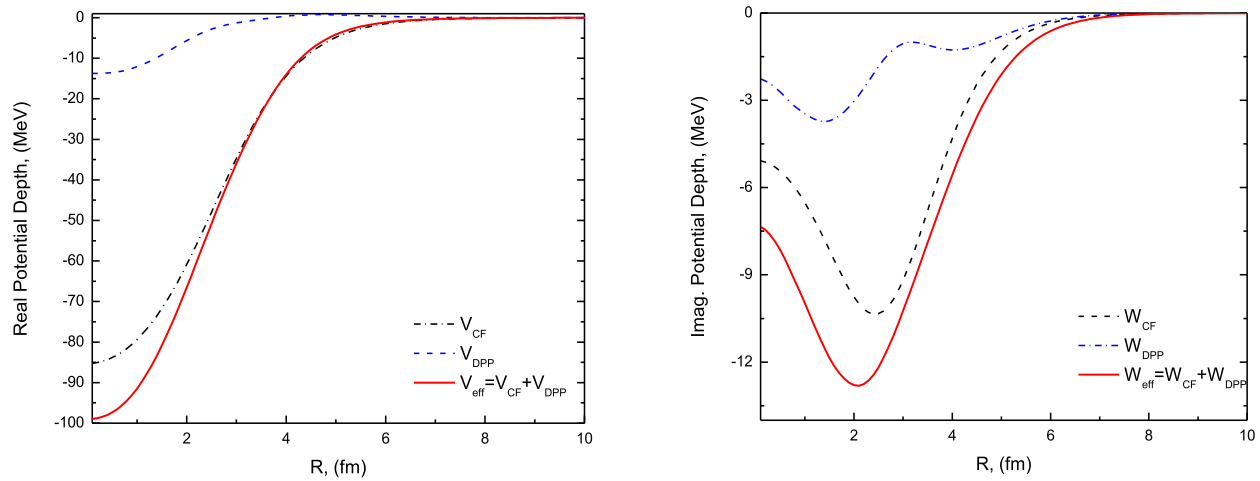

Fig. 2. (color online) Generated effective potential ($U_{\rm eff}$) from the microscopic CDCC calculations

Ref. [18] to ensure a meaningful comparison of *SA*s. For the entrance d + ^{11}B channel, we utilized the previously generated $U_{\rm eff}$ (see Fig. 2) without any renormalizations, maintaining consistency with the breakup analysis. For the exit p + ^{12}B channel, we employed the potential of Liu *et al.* [33] without modification. This potential was originally constrained by elastic scattering data at nearby energies and has been used successfully in a previous (d, p) study [18]. Therefore, we adopt it without further adjustment, avoiding the potential ambiguities associated with searching on exit channel parameters. The binding potentials for the overlaps followed the same conventions as in Ref. [18]: a Gaussian potential for the n + p (deuteron) system with V_0 = 72.15 MeV and r_0 = 1.484 fm, and Woods-Saxon potentials for the n + ^{11}B overlaps with r_0 = 1.25 fm and a_0 = 0.65 fm, with depths adjusted to reproduce the neutron binding energies of the respective ^{12}B states.

Figure 3 compares the experimental ADs for the ^{11}B(d, p)^{12}B reaction leading to the four aforementioned ^{12}B states with our CRC calculations. The theoretical curves, shown as solid lines, demonstrate reasonably good agreement with the measured cross sections across the entire angular range. The (2$^+$, 0.953 MeV)^{12}B state was assigned a 3P$_{1/2}$ configuration in Ref. [18], which is not credible for such a light system. Shell-model calculations by Cohen and Kurath [34] indicate that this state should be a mixture of 1P$_{3/2}$ and 1P$_{1/2}$, with a dominant 1P$_{1/2}$ component. Therefore, we have considered the (d, p) cross section for this state assuming a pure 1P$_{1/2}$ configuration.

The optimal *SA*s for the configurations: ^{12}B$_{(1^+,\,0.0)}$ → ^{11}B + n, ^{12}B$^*_{(2^+,\,0.953)}$ → ^{11}B + n, ^{12}B$^*_{(2^-,\,1.674)}$ → ^{11}B + n , and ^{12}B$^*_{(0^+,\,2.72)}$ → ^{11}B + n were derived by fitting the experimental data across the full angular range while minimizing χ^2/N, as illustrated in Fig. 4. The extracted *SA* values, presented in Table 3, are in good agreement with those previously reported in Ref. [18] where available, with the exception noted above. Regarding the quality of fits, the (2$^-$, 1.674 MeV) state yields $\chi^2/N \approx 104$, with a calculated diffraction minimum near 20° that is absent in the data; therefore, the *SA* for this state should be regarded as indicative rather than definitive. For the remaining states, χ^2/N values are in the range 2.5−10.5,

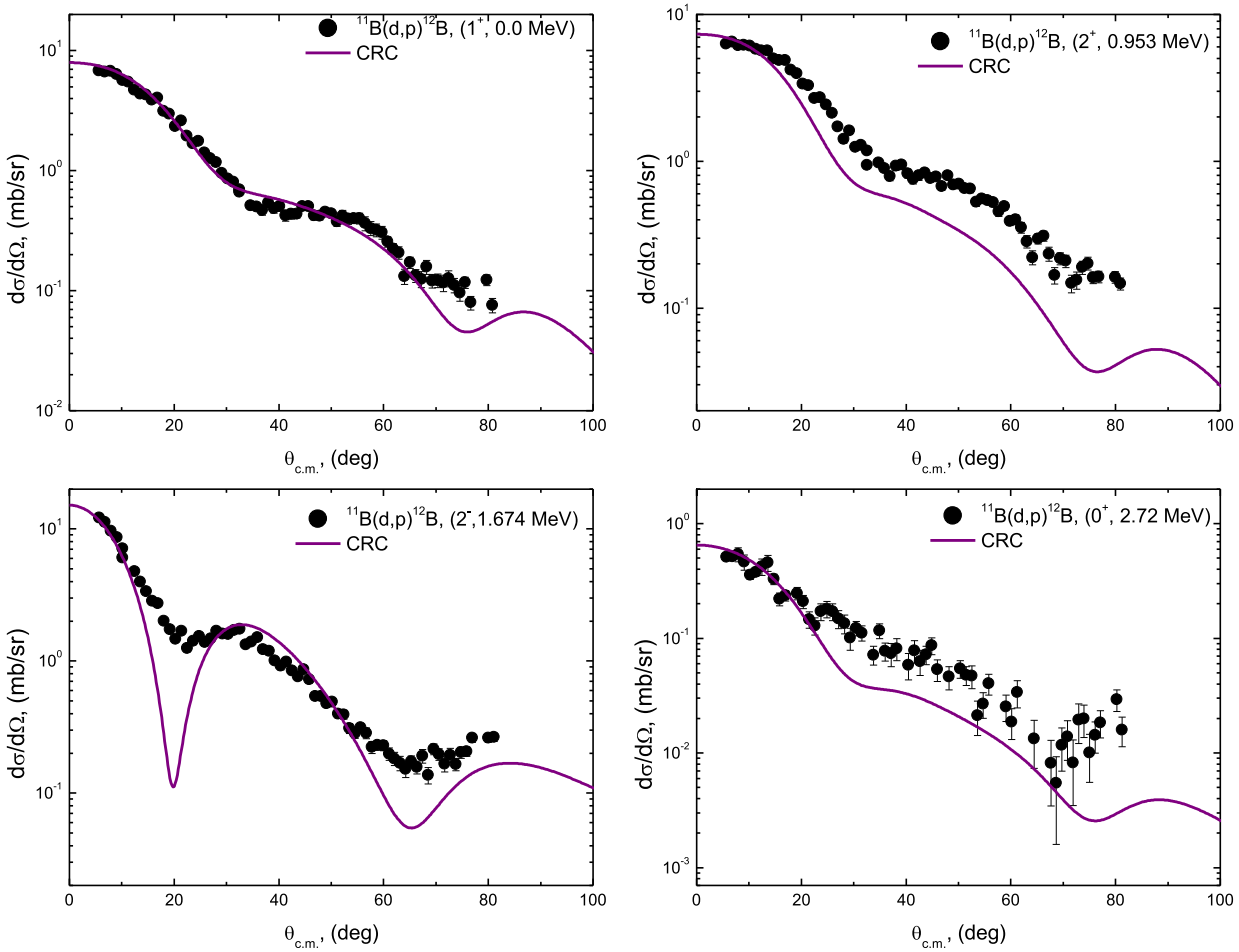

Fig. 3. (color online) Measured ADs for the ^{11}B(d, p)^{12}B reaction at $E_{\rm lab}$ = 21.5 MeV populating the (1$^+$, 0.0 MeV), (2$^+$, 0.953 MeV), (2$^-$, 1.674 MeV), and (0$^+$, 2.72 MeV) states of ^{12}B (circles) compared with CRC calculations (curves)

Table 3. List of *SA*s used in the CRC computations for the ^{11}B(*d*, *p*)^{12}B, ^{11}B(*d*, *t*)^{10}B, and ^{11}B(*d*, ^{3}He)^{10}Be reactions. The asterisks denote *SA* values that were fixed according to literature data.

Configuration	*nLj*	*SA* (P.W.)	Ref.
	$1P_{1/2}$	0.374*	[18]
$^{12}B_{(1^+, 0.0)} \rightarrow {}^{11}B + n$	$1P_{3/2}$	0.865	This work
$^{12}B^*_{(2^+, 0.953)} \rightarrow {}^{11}B + n$	$1P_{1/2}$	0.549	This work
$^{12}B^*_{(2^-, 1.674)} \rightarrow {}^{11}B + n$	$2S_{1/2}$	0.448	This work
$^{12}B^*_{(0^+, 2.72)} \rightarrow {}^{11}B + n$	$1P_{3/2}$	0.224	This work
$^{3}H \rightarrow d + n$	$1S_{1/2}$	1.2274*	[36]
$^{11}B \rightarrow {}^{10}B_{(3^+, 0.0)} + n$	$1P_{3/2}$	1.05*	[34]
	$1P_{3/2}$	0.27*	[34]
$^{11}B \rightarrow {}^{10}B^*_{(1^+, 0.718)} + n$	$1P_{1/2}$	0.64	This work
$^{3}He \rightarrow d + p$	$1S_{1/2}$	1.2247*	[36]
$^{11}B \rightarrow {}^{10}Be + p$	$1P_{3/2}$	0.39	This work

which is acceptable for CRC calculations at this energy.

The *SA* value for the configurations $^{12}B^*_{(2^+, 0.953)} \rightarrow {}^{11}B + n$ (*SA*= 0.549) is in reasonable agreement with the previously reported theoretical value (*SA*= 0.748) from Ref. [34].

B. Neutron-pickup transfer reaction ^{11}B(*d*, *t*)^{10}B

We next examined how neutron pickup influences the $d + {}^{11}$B elastic scattering channel by analyzing the ^{11}B(*d*, *t*)^{10}B reaction at E_d= 18 MeV [19]. This dataset includes transitions to the following ^{10}B ground state (3^+, 0.0 MeV) and the first excited state (1^+, 0.718 MeV). The CRC calculations for this reaction require optical potentials for both the entrance ($d + {}^{11}$B) and exit ($t + {}^{10}$B) channels, together with *SA*s describing the relevant nuclear overlaps. For the entrance channel, we again employed the non-renormalized $U_{\rm eff}$ derived from our CD-CC calculations. The optical potential for the exit $t + {}^{10}$B channel was adopted from the global triton parameterization of Pang *et al.* [35]. Our CRC calculations for the (*d*, *t*) reaction were performed consistently with the (*d*, *p*) analysis described in Section III. A, using the prior form of CRC with full complex remnant terms and non-orthogonality corrections as implemented in **FRESCO** code.

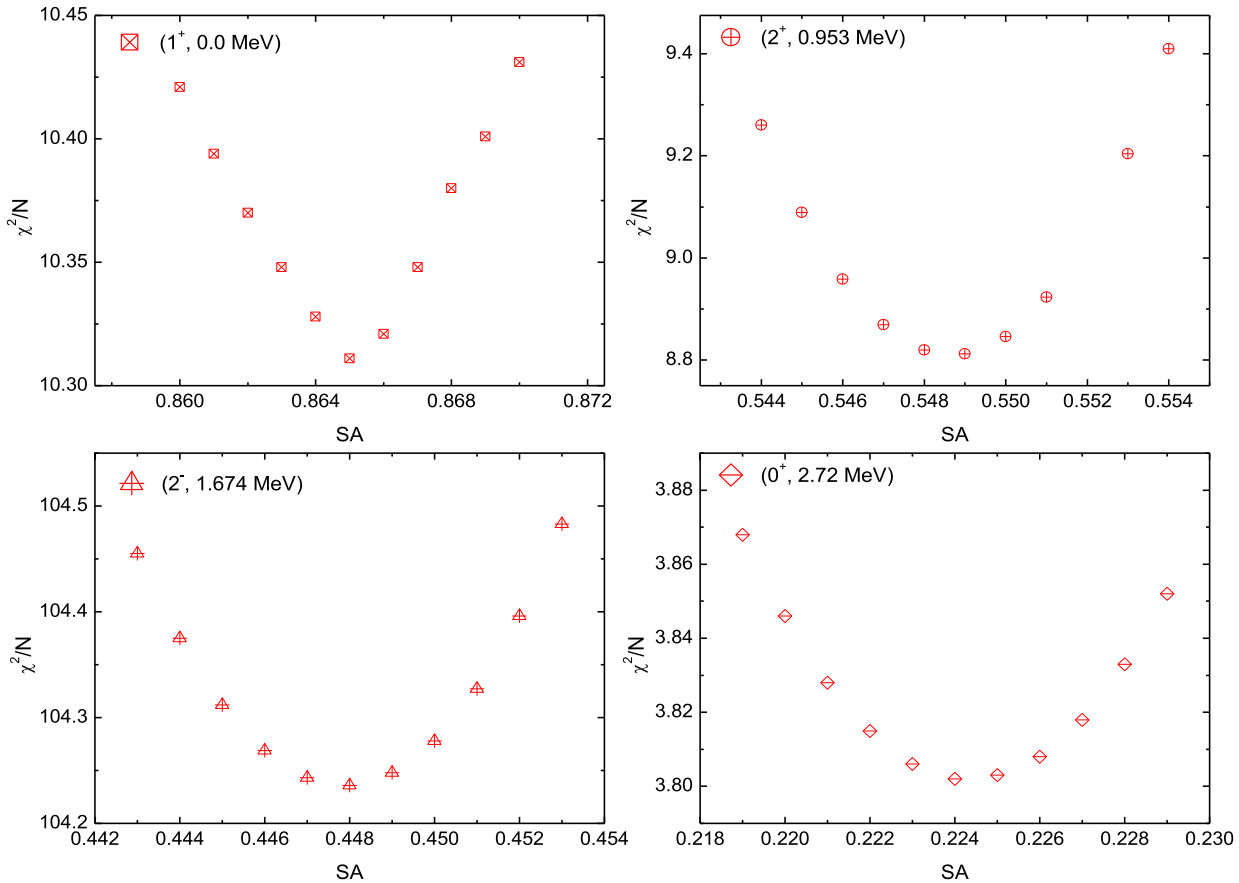

Fig. 4. (color online) Dependence of the χ^2/N value on the extracted *SA*s obtained from CRC computations for the ^{11}B(*d*, *p*)^{12}B reaction at $E_{\rm lab}$= 21.5 MeV. The panels correspond to transitions to the (1^+, 0.0 MeV), (2^+, 0.953 MeV), (2^-, 1.674 MeV), and (0^+, 2.72 MeV) states in ^{12}B.

The binding potentials for the overlaps followed the same conventions as in Ref. [18]: a Woods-Saxon potential for the n + ^{10}B overlaps with r_0 = 1.25 fm and a_0 = 0.65 fm, with depths adjusted to reproduce the neutron binding energies of the respective ^{10}B states.

To obtain an optimal description of the transfer data, we performed a search using the **SFRESCO** code. For the ^{10}B ground state (3^+, 0.0 MeV), the $1P_{3/2}$ component was fixed to the literature value of 1.05 from Cohen and Kurath [34]. For the (1^+, 0.718 MeV) state, the $1P_{3/2}$ component was fixed to 0.27 from the same source, whereas the $1P_{1/2}$ component was varied to fit the data, yielding a value of 0.64, which is in reasonable agreement with the reported value (SA=0.44) from Ref. [34]. The potentials employed for the entrance and exit channels are listed in Table 2. Figure 5 presents a comparison between the experimental ADs for the ^{11}B(d, t)^{10}B reaction at E_d = 18 MeV, populating the (3^+, 0.0 MeV) and (1^+, 0.718 MeV) states of ^{10}B, and our theoretical CRC predictions.

C. Proton-pickup transfer reaction ^{11}B(d, ^{3}He)^{10}Be

Finally, we examined the coupling effects arising from the (d, ^{3}He) proton transfer reaction on the d + ^{11}B elastic scattering channel. To this end, we analyzed previously measured ADs for the ^{11}B(d, ^{3}He)^{10}Be reaction at E_d = 22 MeV, which populate the ^{10}Be ground state [20], using the CRC formalism. For the entrance d + ^{11}B channel, we again employed the non-renormalized effective potential derived from our CDCC calculations. The exit channel ^{3}He + ^{10}Be potential was taken in accordance with Ref. [35]. As in the previous transfer calculations, the CRC calculations were performed in the prior form, including full complex remnant terms and non-orthogonality corrections as implemented in **FRESCO** code. Woods-Saxon type binding potentials, with conventional geometrical values r_0 = 1.25 fm and a_0 = 0.65 fm, were employed to describe the ^{3}He and ^{11}B wave functions. The CRC results were observed to be in reasonable accordance with the measurements of Ref. [20], as displayed in Fig. 6.

To assess the relative importance of different transfer channels on the d + ^{11}B elastic scattering, we performed four calculations: breakup only, breakup+(d, p), breakup+(d, p)+ (d, t), and breakup+(d, p)+ (d, t)+ (d, ^{3}He). These calculations were performed using the potentials listed in Table II and the overlaps given in Table III. In all cases, the previously generated $U_{\rm eff}$ from the CDCC computations (without any renormalization) was employed for the d + ^{11}B entrance channel. As illustrated in Fig. 7, the calculated d + ^{11}B ADs are presented as ratio to Rutherford. The dotted curve shows the breakup-only (CDCC) result. Adding the (d, p) coupling alone (dashed curve) has very little influence on the elastic scattering angular distribution, as it remains close to the breakup-only result (dotted curve). In contrast, the further inclusion of the (d, t) coupling (dashed-dotted curve) produces a significant effect over a broad angular range, from approximately 40° to 100° and also at angles greater than ~130°. The solid curve, which additionally includes the (d, ^{3}He) channel, is almost indistinguishable from the dashed-dotted curve, confirming that the proton pickup contribution is negligible. These findings are consistent with those of Amar *et al.* [14] at 14.5 MeV, where

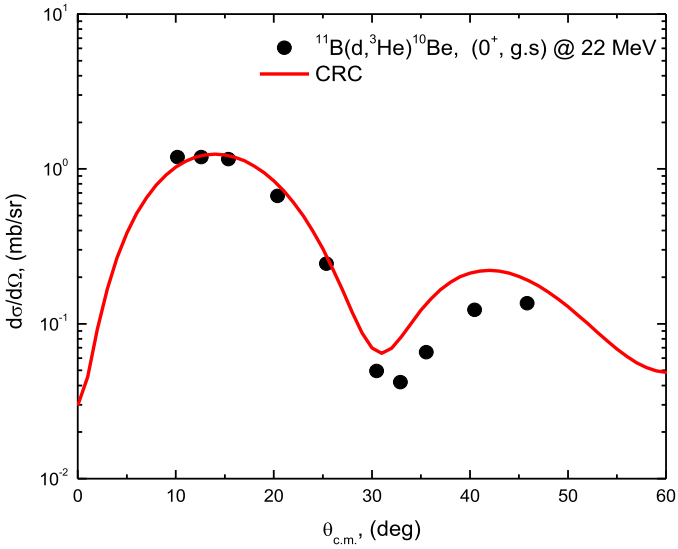

Fig. 6. (color online) Measured ADs for the ^{11}B(d, ^{3}He)^{10}Be reaction at $E_{\rm lab}$ = 22 MeV, populating the (0^+, 0.0 MeV) ^{10}Be ground state (circles), compared with CRC calculations (curves)

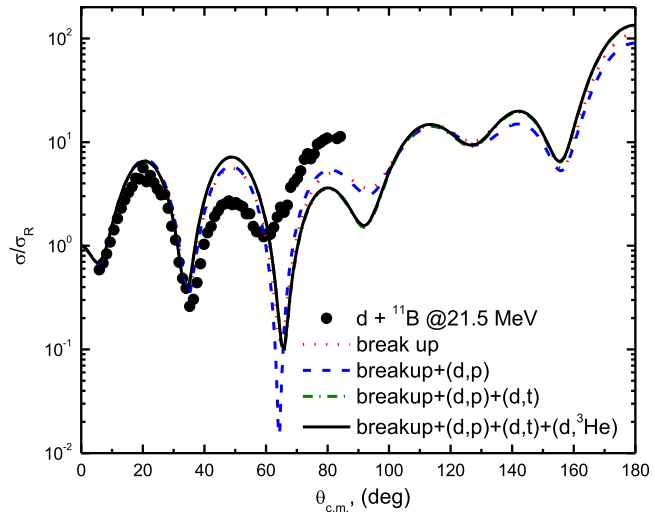

Fig. 7. (color online) Measured ADs for d + ^{11}B elastic scattering at $E_{\rm lab}$ = 21.5 MeV (ratio to Rutherford) compared with CDCC and CDCC+CRC calculations. The different curves correspond to progressively including more reaction channels: dotted – breakup only; dashed – breakup plus (d, p); dashed-dotted – breakup plus (d, p) and (d, t); solid – breakup plus (d, p), (d, t), and (d, ^{3}He).

the (d, t) coupling also dominated and the (d, p) coupling had very little influence. Importantly, none of the calculated curves fully resolve the discrepancies in the intermediate angular region, and the full coupling still overshoots the data in some parts. This indicates that, although the (d, t) transfer channel is necessary to describe the elastic scattering, other missing physics (possibly target excitation or more complex reaction paths) remains important.

IV. SUMMARY

The d + ^{11}B elastic scattering at $E_{\rm d}$ = 21.5 MeV has been analyzed using CDCC and combined CDCC + CRC approaches. Breakup effects, treated within the CDCC framework, are crucial for describing forward-angle scattering. However, a satisfactory description of the full angular range remains challenging. The (d, p) neutron stripping channel has very little influence on the elastic scattering at this energy, whereas the (d, t) neutron pickup channel produces a significant effect over a broad angular range, from approximately 40° to 100° and also at angles greater than ~130°. The (d, ^{3}He) proton pickup channel plays a negligible role. These results confirm the findings of Amar *et al.* [14] at 14.5 MeV: the (d, t) neutron pickup channel dominates the transfer coupling effects on elastic scattering in the d + ^{11}B system, whereas the (d, p) stripping channel has very little influence, even at the higher incident energy of 21.5 MeV.

In a complementary study on the neighboring d + ^{13}C system, Janseitov *et al.* [17] also observed that deuteron breakup alone is insufficient and that neutron stripping plays a major role. However, in contrast to the present results for d + ^{11}B, they observed that neutron pickup (d, t) had only a minor effect, whereas proton stripping (d, n) was significant —differences attributable to the distinct spectroscopic amplitudes of the two targets.

The present analysis demonstrates that a realistic description of deuteron-induced reactions on light nuclei must account simultaneously for breakup and neutron transfer mechanisms, but also highlights that additional effects (*e.g.*, target excitation or multistep processes) likely contribute to the intermediate-angle region. Spectroscopic amplitudes for the following configurations: $^{12}B_{(1^+,0.0)} \rightarrow {}^{11}B + n$, $^{12}B^*_{(2^+,0.953)} \rightarrow {}^{11}B + n$, $^{12}B^*_{(2^-,1.674)} \rightarrow {}^{11}B + n$, $^{12}B^*_{(0^+,2.72)} \rightarrow {}^{11}B + n$, and $^{11}B \rightarrow {}^{10}B^*_{(1+,0.718)} + n$ were extracted and compared with those in literature.

ACKNOWLEDGMENT

A.A. Ibraheem extends his appreciation to the Deanship of Research and Graduate Studies at King Khalid University for funding this work through the Large Research Groups Program under grant number RGP2/14/47.

References

[1] H . G. Rawitscher, Phys. Rev. C **9**, 2210 (1974)
[2] M. Yahiro *et al*., Prog. Theor. Phys. Supp. **89**, 32 (1986)
[3] N. Austern *et al*., Phys. Rep. **154**, 125 (1987)
[4] C. W. Johnson *et al*., J. Phys. G **47**, 123001 (2020)
[5] N. C. Summers, F. M. Nunes, and I. J. Thompson, Phys. Rev. C **74**, 014606 (2006)
[6] R. C. Johnson, P. C. Tandy, Nucl. Phys. A **235**, 56 (1974)
[7] N. K. Timofeyuk, R. C. Johnson, Prog. Part. Nucl. Phys. **111**, 103738 (2020)
[8] P. Chau Huu-Tai, Nucl. Phys. A **773**, 56 (2006)
[9] N. Keeley, N. Alamanos, V. Lapoux, Phys. Rev. C **69**, 064604 (2004)
[10] N. Keeley, R. S. Mackintosh, Phys. Rev. C **77**, 054603 (2008)
[11] N. J. Upadhyay, A. Deltuva, F. M. Nunes, Phys. Rev. C **85**, 054621 (2012)
[12] R. S. Mackintosh, N. Keeley, Phys. Rev. C **76**, 024601 (2007)
[13] M. Kawai, M. Kamimura, K. Takesako, Prog. Theor. Phys. Supp. **89**, 118 (1986)
[14] A. Amar, K. Rusek, Sh. Hamada, Eur. Phys. J. A **59**, 182 (2023)
[15] F. M. Nunes, A. Deltuva, Phys. Rev. C **84**, 034607 (2011)
[16] A. Deltuva, Phys. Rev. C **79**, 054603 (2009)
[17] D. M. Janseitov *et al*., Rev. Mex. Fís. **71**, 031204 (2025)
[18] T. L. Belyaeva *et al*., Phys. Rev. C **98**, 034602 (2018)
[19] I. R. Gulamov *et al*., Program and Theses, in *Proc. 37th Ann. Conf. Nucl. Spectrosc. Struct. At. Nuclei* (Yurmala: USSR Academy of Sciences, 1987), p. 344
[20] R. H. Stokes and P. G. Young, Phys. Rev. C **3**, 984 (1971)
[21] I. Thompson, Comput. Phys. Rep. **7**, 167 (1988)
[22] K. Ogata *et al*., Phys. Rev. C **68**, 064609 (2003)
[23] T. Matsumoto *et al*.,Phys. Rev. C **70**, 061601(R) (2004)
[24] M. Rodríguez-Gallardo et al., Phys. Rev. C 80, 051601(R) (2009)
[25] J. Lei, A. M. Moro, Phys. Rev. C **92**, 044616 (2015)
[26] L. F. Canto *et al*., Phys. Rep. **596**, 1 (2015)
[27] L. J. Titus, F. M. Nunes, G. Potel, Phys. Rev. C **93**, 014604 (2016)
[28] J. A. Cookson and J. G. Locke, Nucl. Phys. A **146**, 417 (1970)
[29] B. A. Watson, P. P. Singh and R. E. Segel, Phys. Rev. **182**, 977 (1969)
[30] Y. Iseri, M. Yahiro and M. Kamimura, Prog. Theor. Phys. Suppl. **89**, 84 (1986)
[31] M. Lacombe *et al*., Phys. Rev. C **21**, 861 (1980)
[32] P. Descouvemont, Phys. Rev. C **97**, 064607 (2018)
[33] Z. H. Liu *et al*., Phys. Rev. C **64**, 034312 (2001)
[34] S. Cohen, D. Kurath, Nucl. Phys. A **101**, 1 (1967)
[35] D. Y. Pang *et al*., Phys. Rev. C **79**, 024615 (2009)
[36] A. T. Rudchik, Yu. M. Tchuvilsky, Ukr. Fiz. Zh. **30**, 819 (1985)